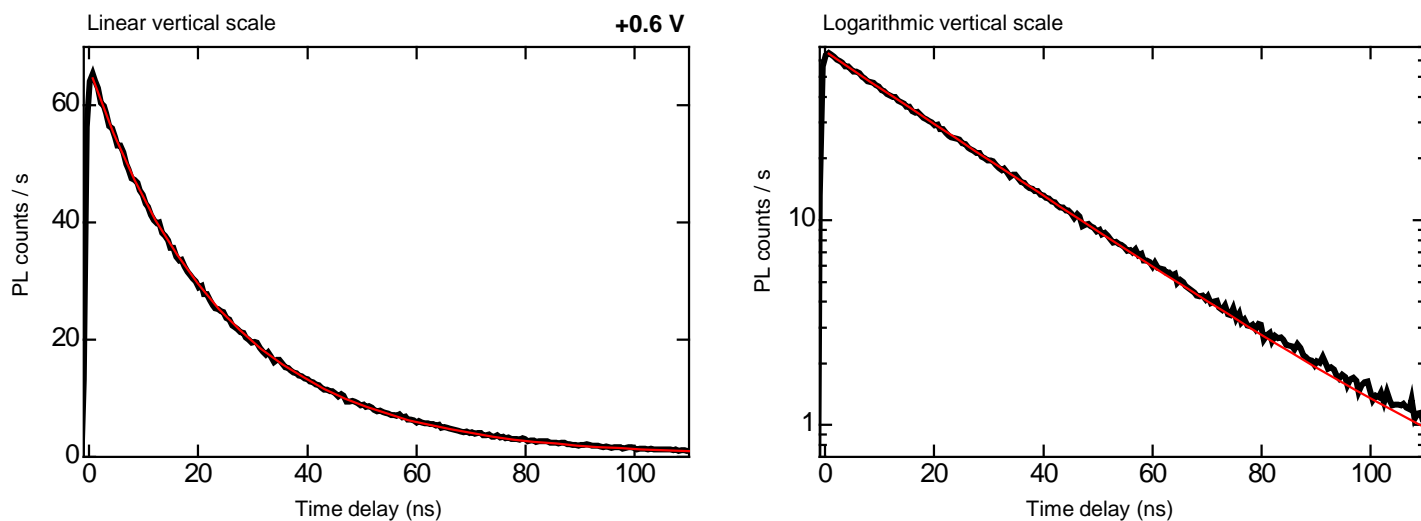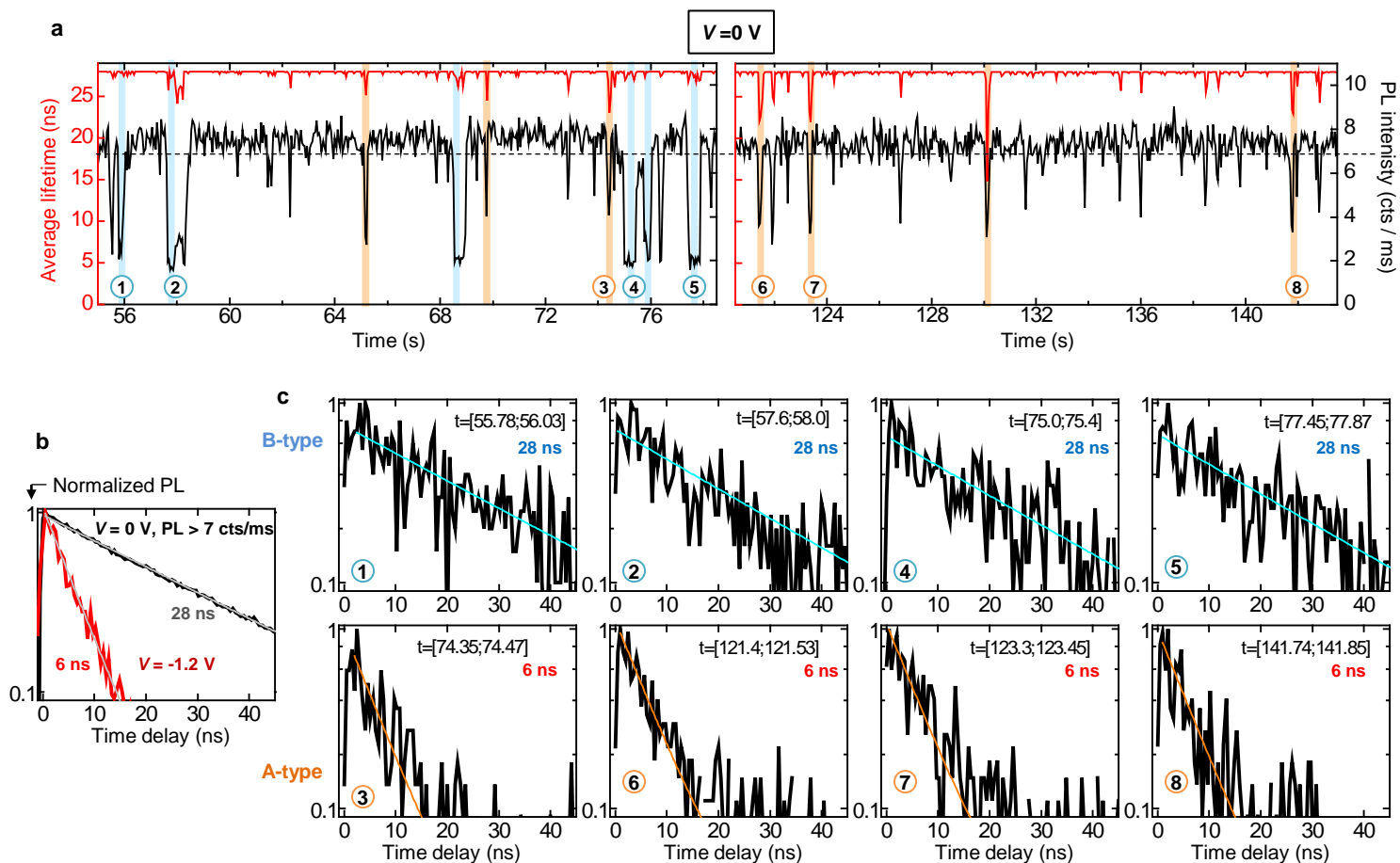**Supplementary Figure 1. Full PL intensity and lifetime trajectories corresponding to Fig. 3 a-b.**

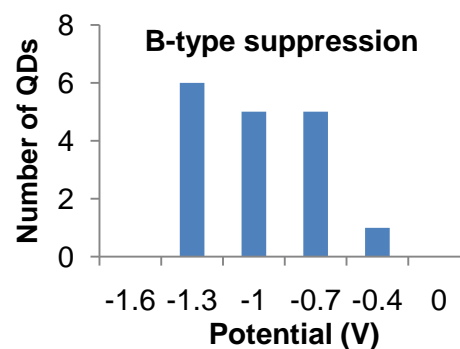**Supplementary Figure 2. Decay curve at +0.6 V for the nanocrystal shown in Fig. 3a.**

Decay curve at +0.6 V for the nanocrystal shown in Fig. 3a (solid black lines). The red line is a mono-exponential fit with time constant 24 ns, evidencing that the emission is originating exclusively from the neutral exciton.

Supplementary Figure 3. Coexistence of A-type and B-type blinking at 0 V.

a, Two portions of the average PL lifetime (blue) and PL intensity (black) trajectories for the nanocrystal shown in Fig. 4a, at $V = 0$ V. The bin size is 50 ms. Some A-type blinking events are highlighted in orange and are characterized by correlated reduction of intensity and lifetime. In contrast, B-type low-intensity periods (some are highlighted in blue) do not correlate with significant change in average lifetime. **b**, Normalized PL decay curves (logarithmic scale) for the ON state at $V = 0$ V (black, obtained by selecting all bins with intensities higher than the threshold shown as a dashed horizontal line in (a)) and for the same nanocrystal at $V = -1.2$ V (red, no threshold). Thin grey lines are mono-exponential fits, with lifetimes 28 ns at $V = 0$ V and 6 ns $V = -1.2$ V, which can be attributed to X^0 and X^-, respectively. **c**, Normalized PL decay curves at $V = 0$ V corresponding to the small time intervals (100 to 400 ms) highlighted and numbered in (a). Red lines are simulated mono-exponential decays (not fits) with either of the lifetimes extracted in (b). The dynamics during B-type low-intensity periods (curves 1, 2, 4 and 5) is similar to the bright, neutral exciton X^0. A-type events (curves 3, 6, 7 and 8) show a decay dominated by the charged exciton X^-, in agreement with the charging model.

nanocrystal	batch	shell ML	ligand	electrolyte	At 0 V		Suppressed at potential (V)	
					A-type	B-type	A-type	B-type
1	256L	7	W	TBA		X		-1
2	256L	7	W	TBA	X	X		
3	256L	7	W	TBA	X	X		-1
4	256L	7	W	TBA		X		-1.2
5	256L	7	W	TBA		X		-0.8
6	256L	7	W	TBA		X		-1.4
7	256L	7	W	TBA	X		1	
8	256L	7	W	TBA		X		-1.2
9	256L	7	W	TBA		X		-1
10	256L	7	W	TBA	X	X		-1
11	256L	7	W	TBA		X		-1.2
12	256L	7	W	TBA		X		-1.4
13	256M	8	H	PC		X		
14	256M	8	H	TBA		X		-0.8
15	256M	8	H	TBA	X	X	0.5	-0.8
16	256M	8	H	TBA	X	X		-1.4
17	256L	7	W	Li	X			
18	218C	9	H	TBA	X	X	0.8	-1
19	218C	9	H	TBA		X		
20	218C	9	H	TBA		X		-0.6
21	218C	9	H	Li	X		0.6	
22	218C	9	H	Li		X		-0.6
23	218C	7	W	Li	X	X		-0.4

A only	3
B only	13
A+B	7
Total	23

A only ■ A+B ■ B only

B-type suppression
Number of QDs vs Potential (V)

Abbreviations:

• W : Water-solube ligands

• H : Native ligands (soluble in hexane)

• TBA : Tetra-butyl-ammonium Perchlorate in Propylene Carbonate

• Li : Lithium Perchlorate in Propylene Carbonate

• PC : Propylene Carbonate only (no supporting electrolyte)

Supplementary Table 1. Statistics on nanocrystals with intermediate shell thickness (7 to 9 MLs).
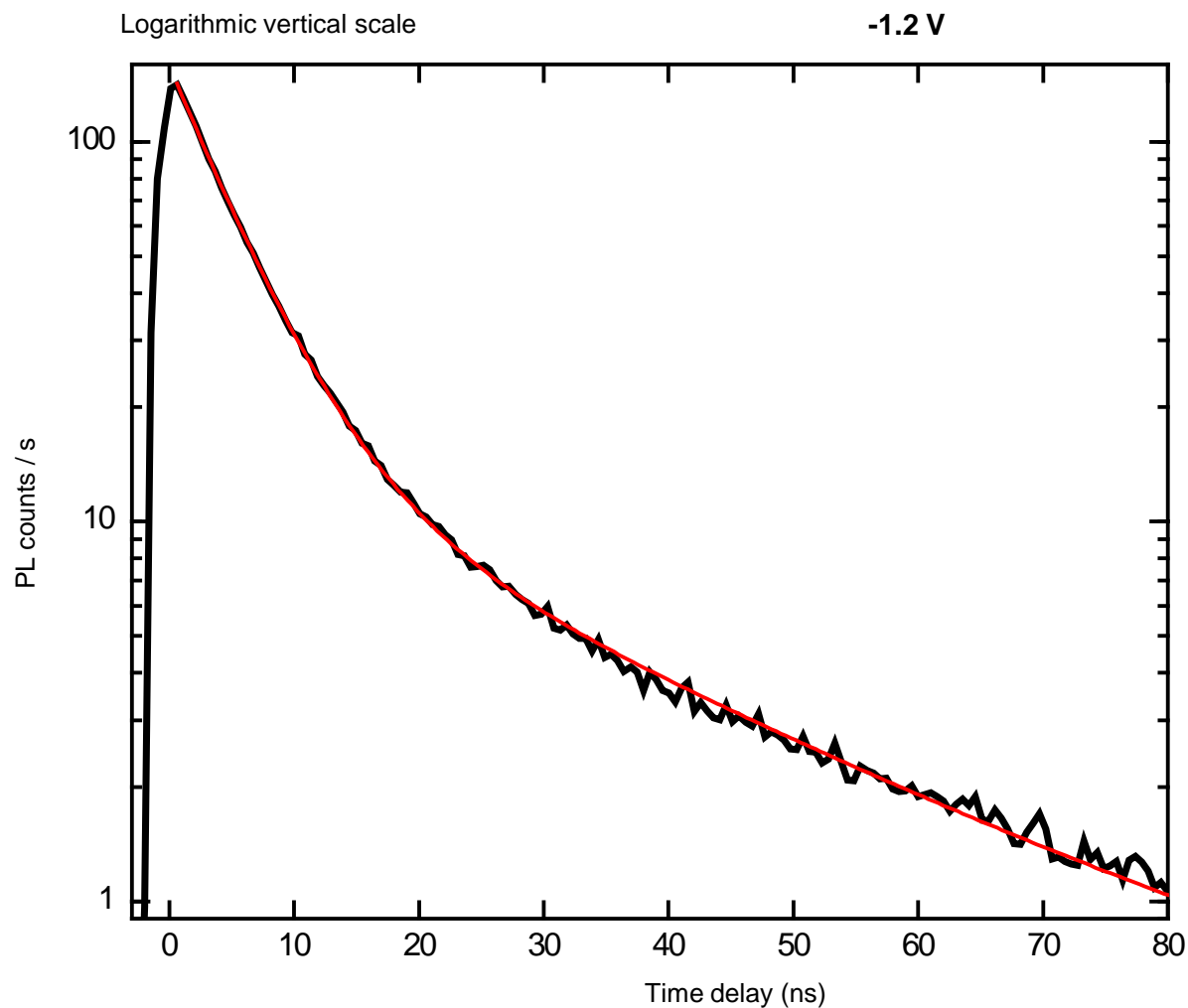
Supplementary Figure 4. Decay curve at -1.2 V for the nanocrystal shown in Fig. 4a.

The PL decay curve (solid black line) for applied potential of -1.2 V for the nanocrystal shown in Fig. 4a. The red line is a biexponential fit with time constants of 6 ns and 28 ns, which yields the average PL lifetime of 12.5 ns seen in Fig. 4a (right). The biexponential decay is a result of very fast switching between the neutral exciton (28 ns lifetime) and the negatively charged trion (6 ns lifetime).
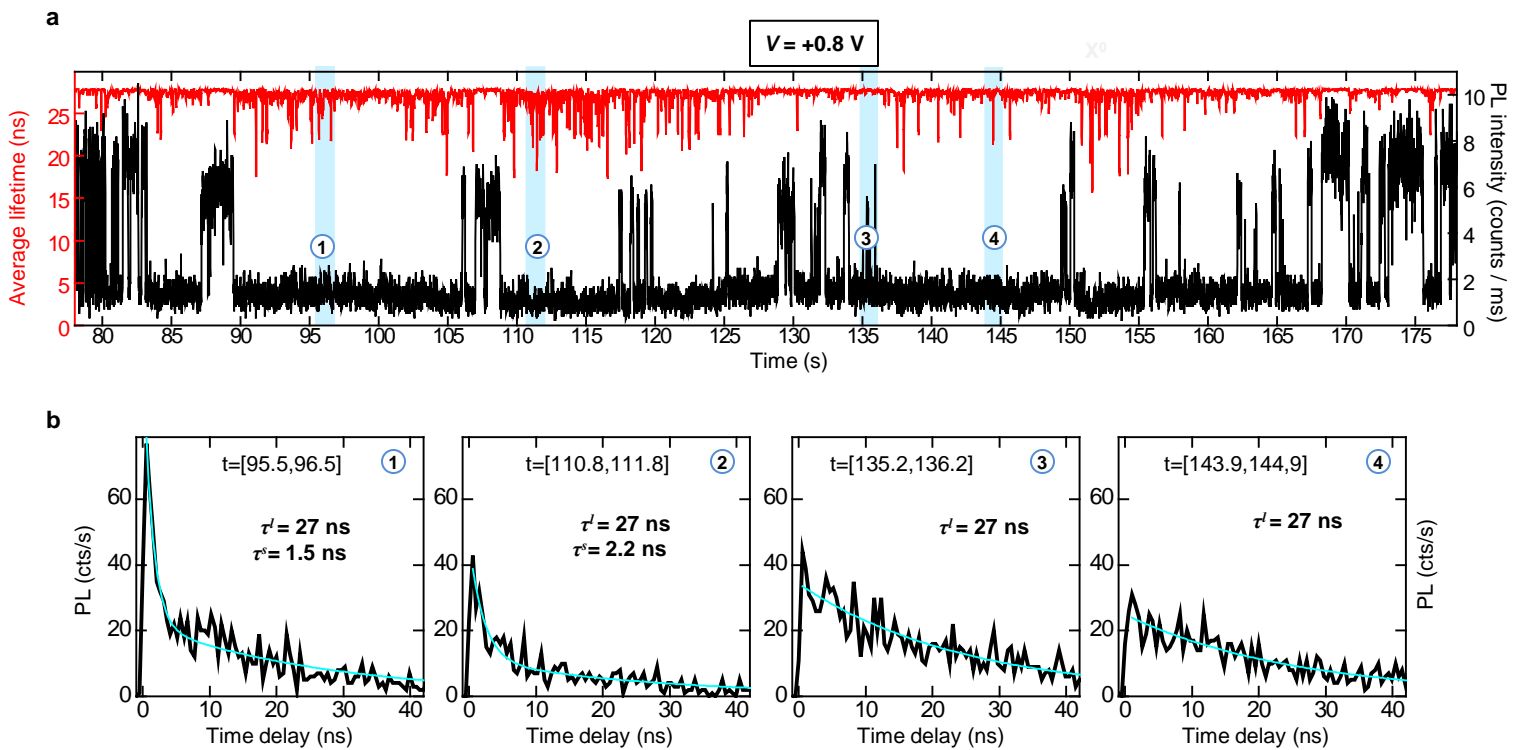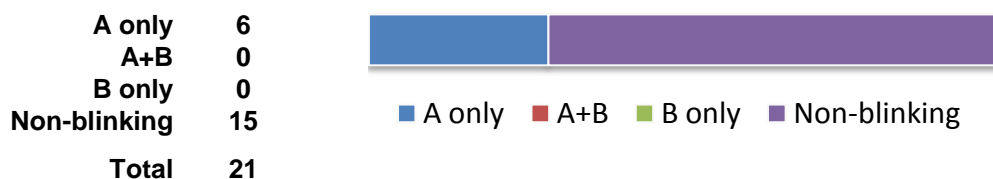
Supplementary Figure 5. Variable PL dynamics within the B-type OFF periods.

a, Portion of the average PL lifetime (blue) and PL intensity (black) trajectories for the nanocrystal shown in Fig. 4a, at $V = +0.8$ V. The bin size is 20 ms. The frequency and length of B-type OFF periods is increased compared to $V = 0$ V. **b**, PL decay curves over 1 s time intervals during OFF periods highlighted and numbered in (a). Thin blue lines are mono- or bi-exponential fits with time constants indicated on the graphs. During most of the OFF periods the decay is quasi-monoexponetial with the lifetime of neutral exciton (~27 ns). But some relatively long intervals like 1 and 2 show an additional fast component of a few nanoseconds. We tentatively attribute this lifetime to positively charged excitons that may form during B-type OFF periods when the captured electrons do not recombine immediately with the hole. The fact that positive trions decay faster than negative trions is not surprising. Auger recombination with excitation of the hole is expected to be more efficient than the processes involving excitation of the electron because the density of valence-band states in II-VI semiconductors is appreciably higher than that of conduction-band states.
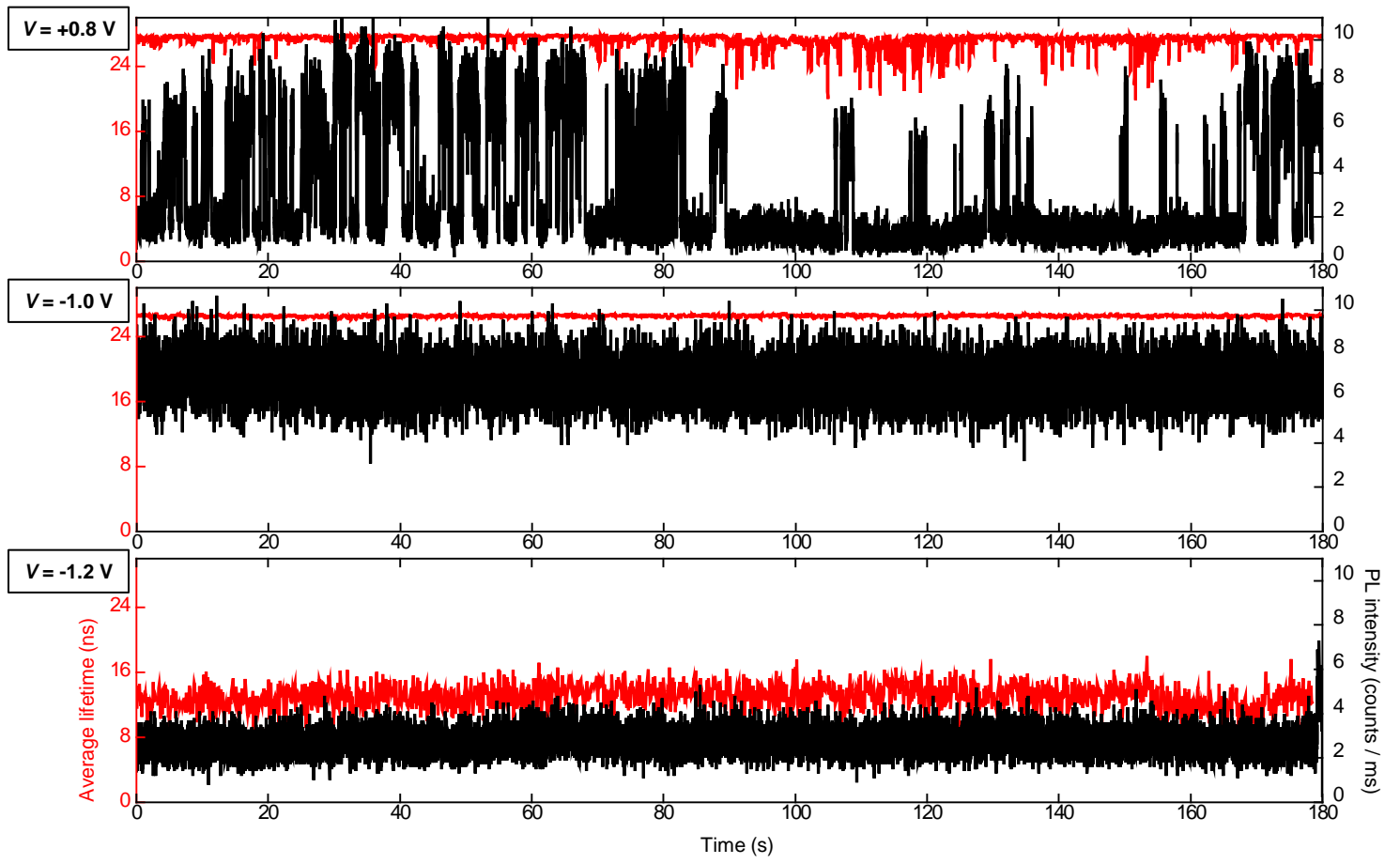
Supplementary Figure 6. Full PL intensity and lifetime trajectories corresponding to Fig. 4a.

nanocrystal	batch	shell ML	ligand	electrolyte	At 0 V Non-Blinking	A-type	B-type
1	216C	15	W	ITO		X	
2	216C	15	W	ITO	X		
3	216C	15	W	ITO	X		
4	216C	15	W	PC	X		
5	216C	15	W	PC	X		
6	216C	15	W	PC	X		
7	216C	15	W	PC	X		
8	216C	15	W	TBA	X		
9	216C	15	W	TBA	X		
10	218C	15	W	Li		X	
11	218C	15	W	TBA	X		
12	218C	15	W	TBA		X	
13	218C	15	W	TBA		X	
14	218C	15	W	Li	X		
15	218C	15	W	Li	X		
16	218C	15	W	Li	X		
17	218C	15	W	ITO		X	
18	218C	15	W	Li		X	
19	218C	15	W	Li	X		
20	218C	15	W	Li	X		
21	218C	15	W	Li	X		

A only	**6**
A+B	**0**
B only	**0**
Non-blinking	**15**
Total	**21**

■ A only ■ A+B ■ B only ■ Non-blinking

Abbreviations:

• W : Water-solube ligands

• H : Native ligands (soluble in hexane)

• ITO : On ITO-coated glass without solvent/electrolyte

• TBA : Tetra-butyl-ammonium Perchlorate in Propylene Carbonate

• Li : Lithium Perchlorate in Propylene Carbonate

• PC : Propylene Carbonate only (no supporting electrolyte)

**Supplementary Table 2. Statistics on nanocrystals with thicker shells (~15 MLs).**
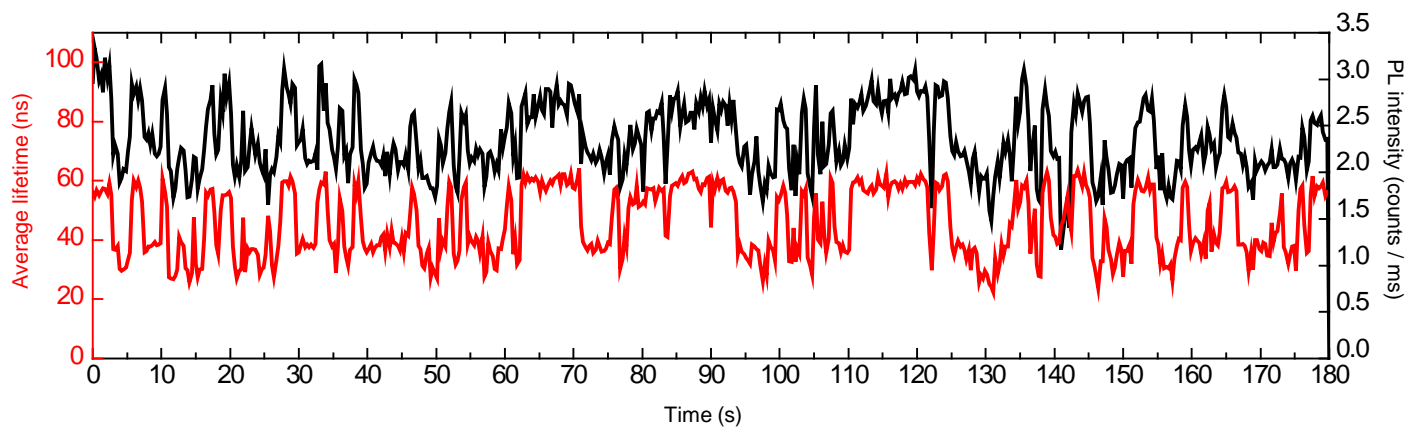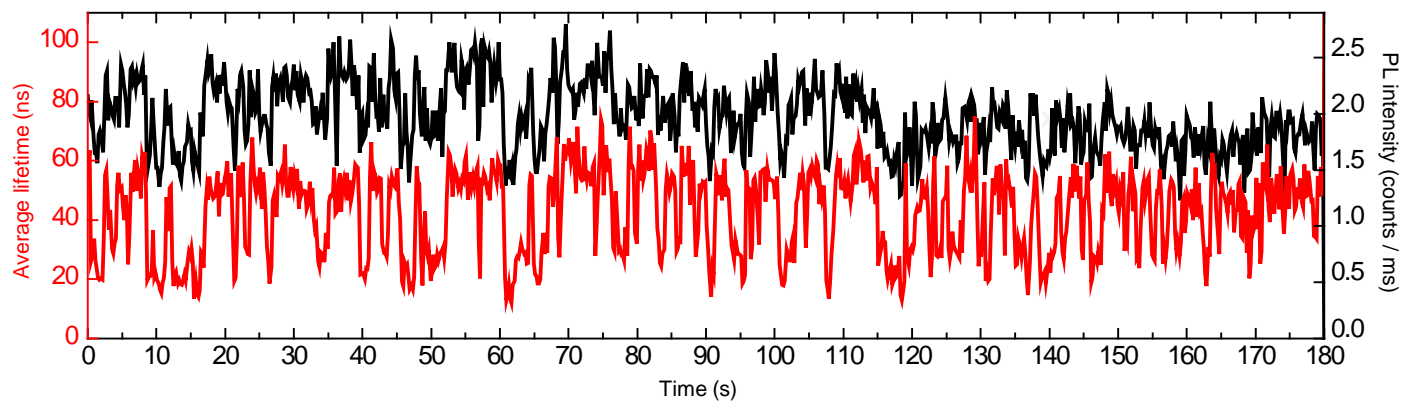
Supplementary Figure 7. A-type blinking in thick shell nanocrystals (15 MLs).

Example of PL lifetime and intensity trajectories for two different 15 ML shell nanocrystals at 0 V, showing only A-type fluctuations. Bin size = 200 ms. The lifetime is evaluated by a weighted average of the micro-time delay for each bin. See also Supplementary Table 2 for complete statistics on 15 ML shell nanocrystals.
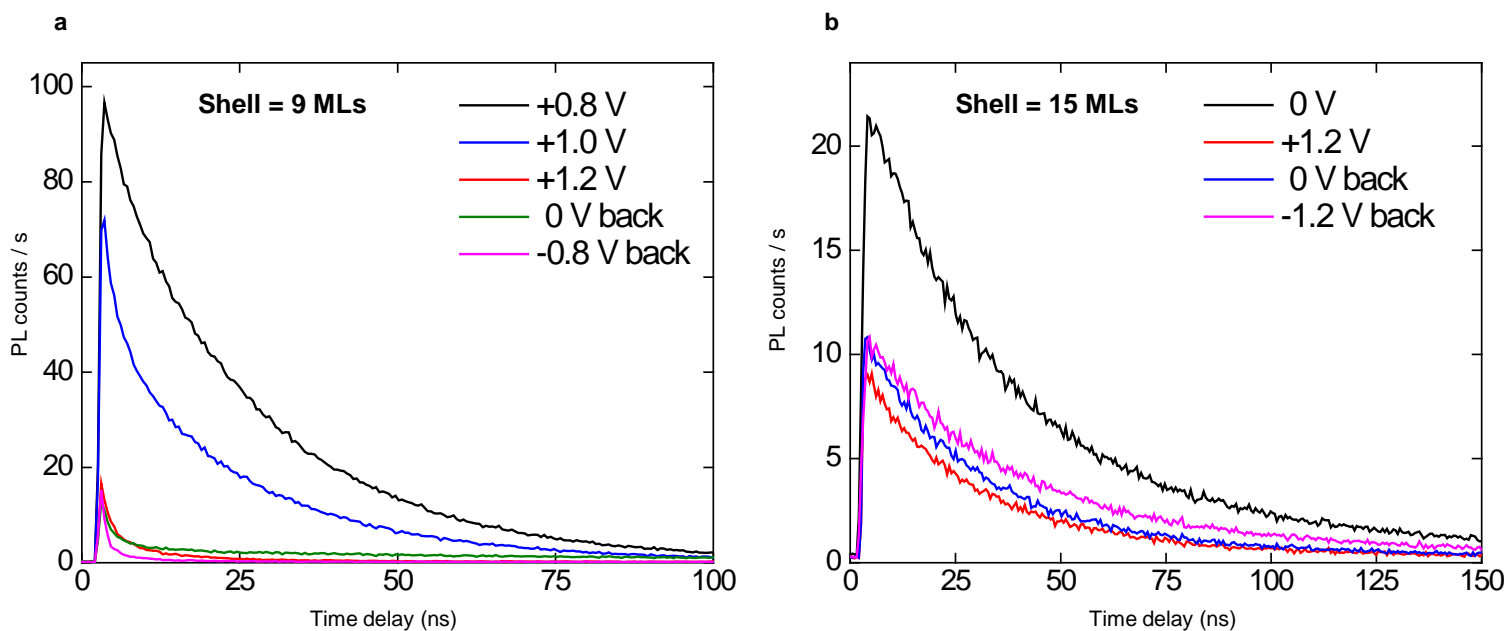
**Supplementary Figure 8. Irreversible quenching at large positive potentials.**

a, Decay curves under increasing positive potential and subsequently back to neutral and negative potential for the nanocrystal shown in Fig. 3 (data shown here taken after the one in Fig. 3). PL is irreversibly quenched by two orders of magnitudes. **b,** Similar experiment on a thicker shell nanocrystal (15 ML). The quenching is also irreversible, but its magnitude is much weaker. This support our arguments for the activation of hot-electron traps at positive potential. This process should indeed be exponentially suppress by increasing the shell thickness because of the reduction of the wavefunction overlap with the surface states. In addition, more experiments on 15-ML shell nanocrystals have shown the absence of B-type blinking under neutral potential in all the nanocrystals we studied. (see Supplementary Table 2 and Supplementary Figure 8).
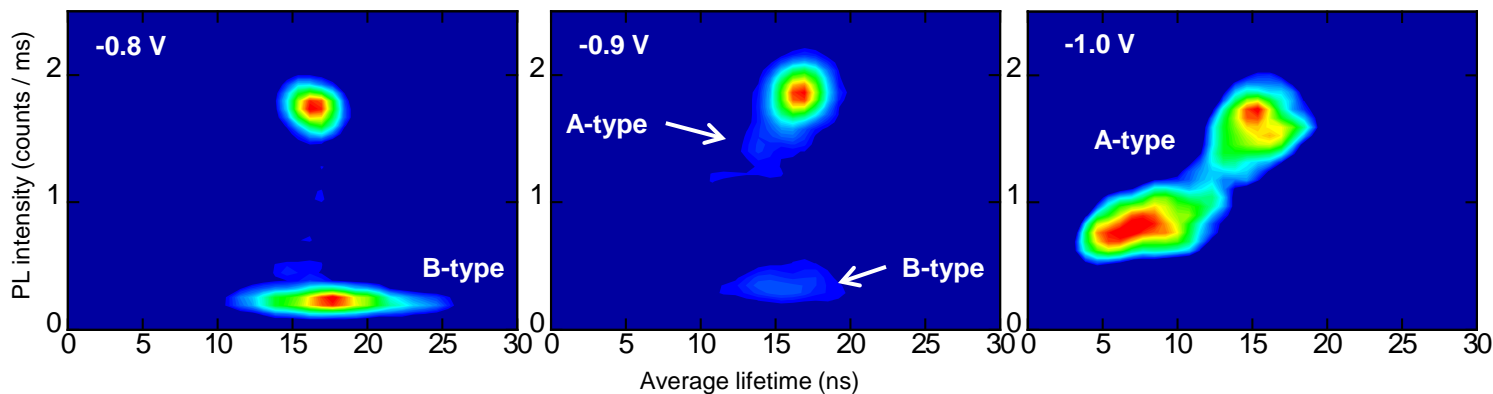
**Supplementary Figure 9. Another example of A/B-type blinking control by electrochemical potential.**

FLIDs from a nanocrystal with 7 MLs CdS shell in water-soluble ligands (see Methods) at three different potentials. At -0.8 V, the nanocrystal is in a strong B-type blinking regime. At -0.9 V B-type events are much less frequent but A-type fluctuations appear.. At -1.0 V, blinking is completely A-type (fluctuations between the neutral and negatively charged exciton).

These FLIDs were constructed using a bin size of 20 ms. For each bin the PL lifetime was calculated by a weighted average of the decay histogram ("micro-times" values). This method does not rely on a fitting procedure but gives results similar to the one presented in Fig. 3 and 4, thus confirming the robustness of our analysis. The main limitation here is that no offset can be accounted for before evaluating the lifetime. Therefore the flat background due to dark counts leads to an overestimate of the lifetime when PL counts are low, as in the B-type state at -0.8 V.
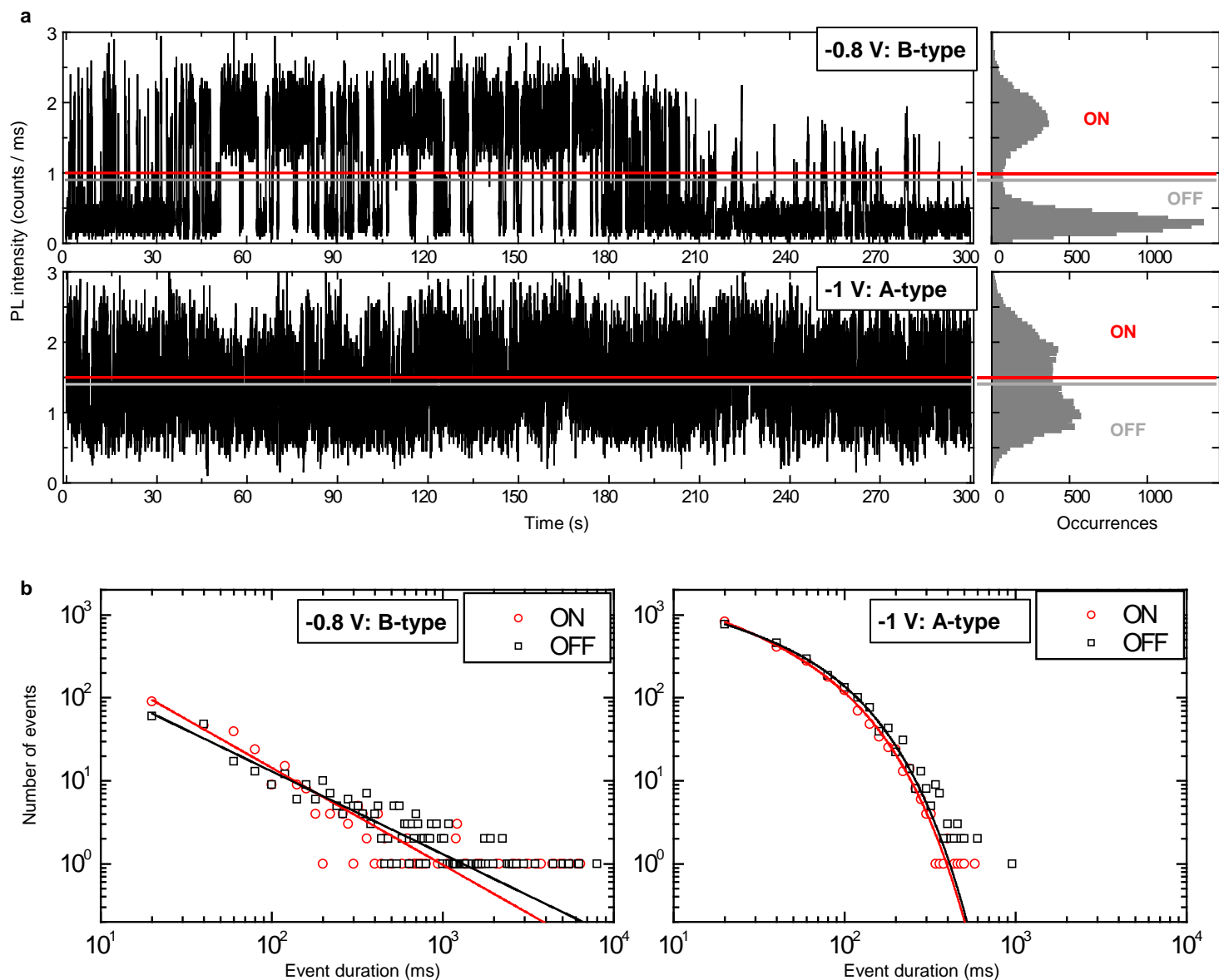
Supplementary Figure 10. Different statistics for A vs. B-type ON/OFF times in the same nanocrystal.

a, PL intensity time trace and occurrence histogram for the nanocrystal shown in Suppl. Fig. 9 at two different potential at which the nanocrystal is either in B-type (-0.8 V) or A-type (-1 V) blinking mode. The bin size is 20 ms. **b,** Corresponding probability densities of ON (red circles) and OFF (black squares) event durations. The thresholds are indicated in (**a**) by red (ON) and grey (OFF) lines. The data at -0.8 V are fitted by pure power laws with exponents -1.17 (ON, red line) and -1.00 (OFF, black line). At -1 V, we need to introduce an exponential cut-off to the power law to fit the experiment. The exponent are -0.54 (ON, red line) and -0.37 (OFF, black line), whereas the cut-off times are 73.4 ms (ON) and 70.8 ms (OFF). The qualitative difference in the ON/OFF times statistics for A and B-type blinking in the same nanocrystal highlights the fundamentally distinct nature of their mechanisms.
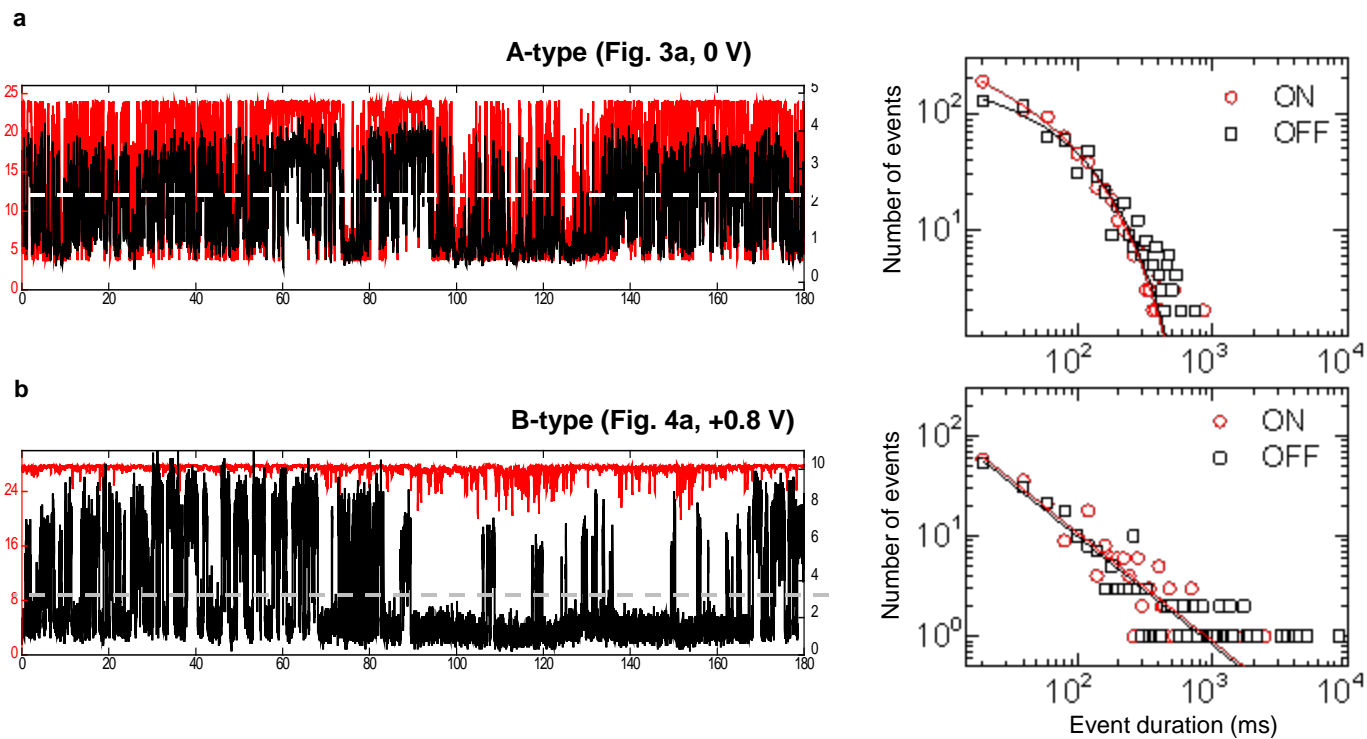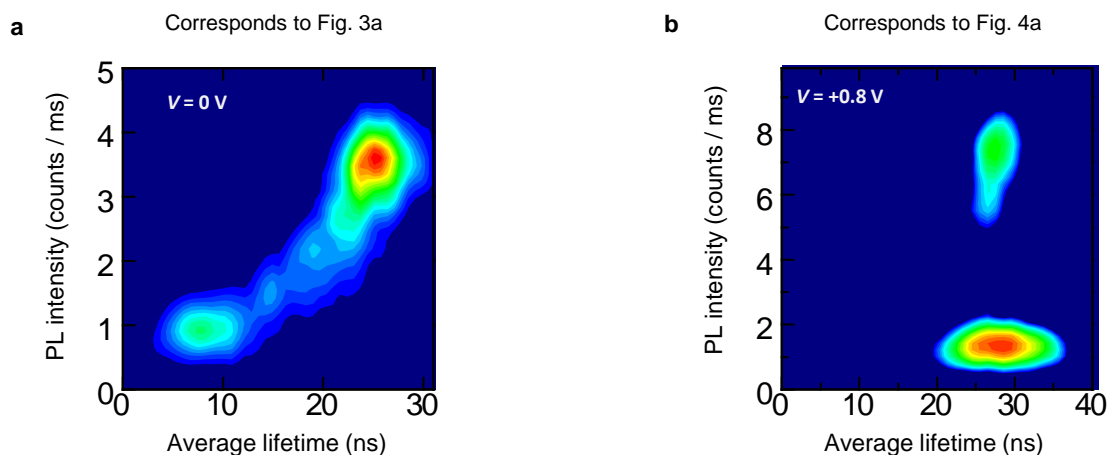
Supplementary Figure 11. ON/OFF times statistics for the nanocrystals in Figs 3 and 4.

a, PL time trace and corresponding ON/OFF event duration statistics for the nanocrystal in Fig. 3a at 0 V showing exclusively A-type blinking. The best fits (solid lines) are obtained with exponents -0.42 (ON) and -0.20 (OFF), and exponential cutoff times 111.5 ms (ON) and 104.6 (OFF). **b,** Same analysis on the nanocrystal of Fig. 4a at +0.8 V, showing only B-type blinking. The solid lines are the best fitted pure power laws with exponents 1.08   0.02 (both ON and OFF). All statistics were calculated with a 20 ms bin; the thresholds discrimating OF/OFF levels are displayed on the time traces on the left.
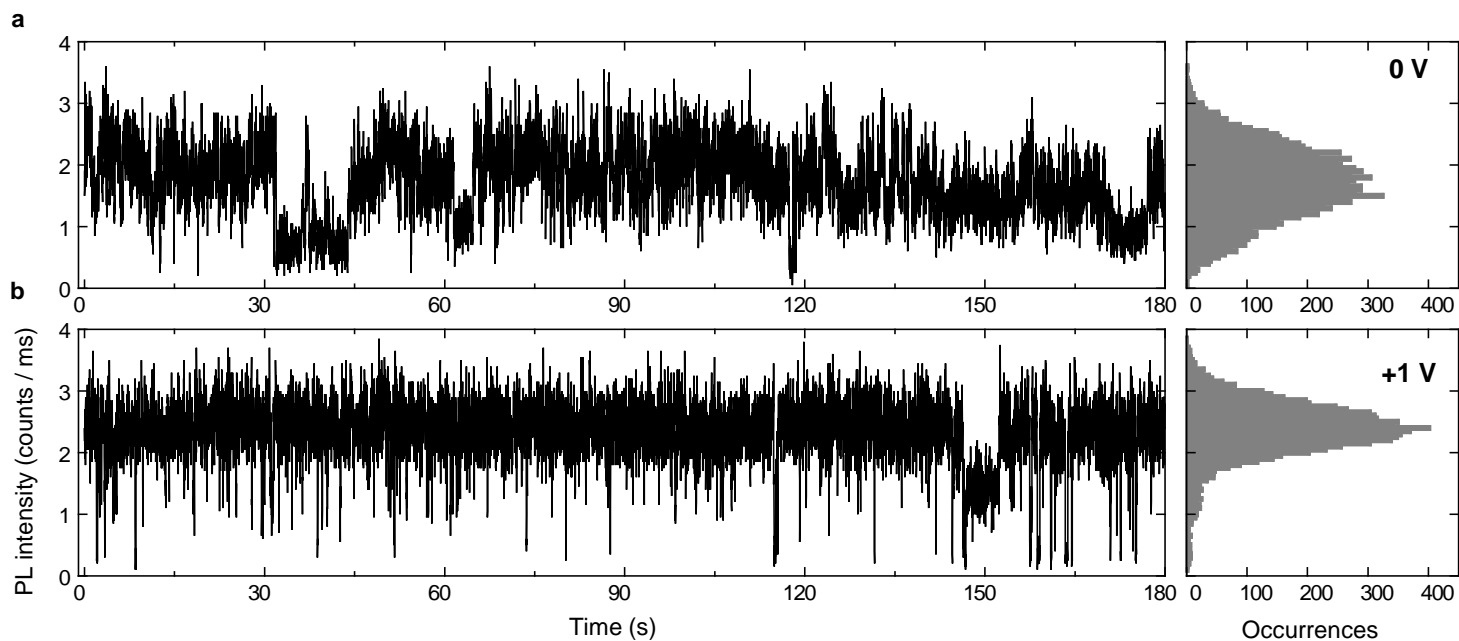
Supplementary Figure 12. An example of A-type flickering suppressed at +1 V.

PL intensity time trace and corresponding distribution histogram at 0 V **(a)** and +1 V **(b)**, showing that fast A-type fluctuations can be significantly reduced under positive potential. The binning time is 20 ms. The nanocrystal is number 7 in Supplementary Table 1.

a Corresponds to Fig. 3a

V = 0 V

PL intensity (counts / ms)

Average lifetime (ns)

b Corresponds to Fig. 4a

V = +0.8 V

PL intensity (counts / ms)

Average lifetime (ns)

Supplementary Figure 13. Validity and robustness of the fitting procedure used in the main text to identify A- and B-type blinking.

FLIDs from the nanocrystals presented in (**a**) Fig. 3a and (**b**) Fig. 4a re-constructed with a "weighted average" lifetime algorithm. As explained in Supplementary Fig. 9, for each time bin, we evaluate the PL lifetime by calculating a weighted average of PL photon arrival times . This method does not rely on any fitting procedure. Importantly, it yields results that are similar to those presented in the main text. This supports the validity of the multiexponential approach used in the present study.